Critical dimension where the macroscopic definition of refractive index can be applied at a nanometric scale

Vincent LeBihan,[1] Anne Pillonnet,[1] David Amans,[1] Gilles Ledoux,[1] Olivier Marty,[2] and Christophe Dujardin[1,*]
[1]*Université de Lyon, Lyon F-69003, France and Laboratoire de Physico-Chimie des Matériaux Luminescents, Université Lyon 1, CNRS UMR 5620, Bât. Kastler, 10 rue Ampère, Villeurbanne F-69622, France*
[2]*INL Institut des Nanotechnologies de Lyon UMR 5270, CNRS-UCBL-INSA-ECL, Bât. Léon Brillouin, Université de Lyon, Villeurbanne F-69622, France*
(Received 3 June 2008; published 9 September 2008)

This Brief Report reports a measurement of the critical dimension where the macroscopic definition of refractive index could be applied at nanometric scale. A fluorescent nanolayer is used as a local probe of the refractive index via its radiative lifetime. By covering the emitting layer with nanofilms of high refractive index material the sphere radius R in which the effective-medium theory has to be applied is estimated as $\lambda/4$ in air.

DOI: 10.1103/PhysRevB.78.113405 PACS number(s): 78.20.Ci, 77.55.+f

In the case of nanomaterials, the refractive index, which is a macroscopic quantity, is hard to define. In particular, one does not know what is the typical size for which an object can be considered as homogeneous regarding this optical parameter. This is particularly important in the case of nanostructures where one has to design complex optical systems composed of materials with various refractive indexes or when single-particle spectroscopy is performed. Indeed, in this latter case, the estimation of the effective index of refraction will depend on the particle size and on a finite volume embedding the nanoparticle.

The Clausius Mossotti relation connects a microscopic quantity, the polarizability, to a macroscopic quantity, the dielectric response of matter. The passage from microscopic to macroscopic scale can be shown[1,2] by regarding the macroscopic electrodynamics equations as the volume averaging of microscopic relations. This approach was initially developed in 1895 by Lorentz to define the relevant fields in electromagnetism.[3] The macroscopic Maxwell equations are then derived from the local expression of the fields using the microscopic quantities. This method was taken again and detailed by G. Russakoff in 1970.[2] The spatial average uses a weighting function, which in the simplest model is a rectangular function and is realized in a finite volume characterized by a distance d. This distance must fulfill two criteria: (i) it must be larger than the lattice constant a and (ii) it must be smaller than the wavelength λ. These criteria correspond to the quasistatic case for which the time dependence can be ignored.[2] $a \ll \lambda$ is already satisfied for visible light. The criterion $d \gg a$ is easy to understand but the justification of the criterion $d \ll \lambda$ is more evasive. The main objective of the present paper is to obtain an experimental estimation of d. This problem is similar to the case of mixed effective media since one has to define a critical distance of influence of the index of refraction. Therefore this question reappeared at the end of the 1980s when many models predicting bounds to average fields in two-component composites were described.[1,4,5] Most of them were established in the quasistatic limit (long-wavelength) such as effective-medium models (EMA). The restriction of the effective optical index to a region of the complex plane is improved when the details of the composite are known, i.e., the volume, the shape, and the polarizability of the different constituent phases. In such models, the volume averaging of the microscopic relation between the electric field and the displacement fields requires some conditions. Aspnes[6] wrote, "that the individual grains or regions must be large enough (up to 1–2 nm) to possess their own dielectric identity, but small (down to $0.1\lambda-0.2\lambda$) compared to the wavelength of light." The second criterion was argued in Ref. 7, where the optical index of Al_2O_3 powder was measured for various particle diameters to wavelength ratios. Egan[7] and Aspnes[5,8] showed that it is necessary to consider a finite wavelength model when the characteristic dimensions of the structure are larger than $0.25-0.5\lambda$. The striking point is that the distance d defined previously should be 1–2 nm for Aspnes. The purpose of this contribution is to show that d is significantly larger.

To measure experimentally the minimal distance d on which the optical index is defined, a local probe has been used: a fluorescencing emitting nanolayer whose emission decay time is sensitive to its host refractive index. The nanolayer is covered by a high refractive index passive material whose thickness is controlled on a nanometric scale. Thus, the probe can be considered as local only in one direction. This proposed method is very efficient to fix certain experimental parameters while varying the dielectric surrounding media thickness.

In the weak-coupling regime, Fermi's golden rule is driven by the density of states and the atom-field interaction Hamiltonian H. This simplified model is suitable for spontaneous emission in free space or for an emitter in a low quality factor cavity. H is simply the product between the electric dipole and the average local field. The emission probability of an emitter embedded in a dielectric host is a function of the host refractive index. In a simplified way,[9] the host refractive index n appears (i) through the density of states and (ii) through the normalization of the field in the interaction Hamiltonian. By measuring the decay time of dye molecules,[10] quantum dots,[11] or doped nanoparticules[12,13] in various liquid or polymers having different refractive indexes, the dependence of the radiative decay time versus the refractive index has been clearly demonstrated. In all these papers, it is generally admitted that the effect of the surrounding media extension is less than λ. Furthermore

Yablonovitch *et al.*[14] have observed that the spontaneous emission rate of a thin layer was modified by the refractive index of the substrate.

Other effects can lead to a change in lifetimes. For instance, a multilayer structure can generate local perturbations of the electric field as observed for emitters in a microcavity,[15] near a mirror,[16] or in stratified materials.[17] The sample could be regarded as a plane cavity. We must thus show that a possible cavity effect is negligible in the present case. Both interfaces, between air and titanium oxide and between the gadolinium oxide and the substrate, can be regarded as mirrors. Moreover, both oxide layers can be considered as a single layered cavity since their optical indexes are very close. The quality factor of such cavity is very low, close to 0.5, in view of the weakness of the mirror reflectivities which are, respectively, 11% and 1% (in intensity). For a plane cavity made up of perfect metal mirrors, the maximum of the enhancement corresponds to a reduction by a factor 3 of the lifetime[18] for an optical thickness of the cavity equal to a half wavelength. This factor falls to 1.4 for high quality distributed Bragg reflectors (DBR) with dielectric layers.[19] Many authors expected to observe the enhancement of spontaneous emission.[15] In their optimized devices, the observed enhancement varies between 1.2 and 2. However, the quality factors of their cavities are greatly higher than in our system. Moreover, most of them use a lateral confinement, such as the whispering gallery mode in micropillar, in order to partly eliminate the leakage modes. It is thus clear that in our case the effect must be negligible compared to the optical index effect.

Experimentally, one of the key points is to avoid the change of the nonradiative probability when additional layers are deposited. For this reason, we selected a well-known crystallized $Eu^{3+}:Gd_2O_3$ material as the emitting layer[20] prepared by a sol-gel dip-coating process with heat treatment at 800 °C. The high refractive index passive material is amorphous TiO_2 layers deposited with the same technique at 200 °C.[21] So, as additional layers are deposited, no severe thermal treatments on the $Eu^{3+}:Gd_2O_3$ layer are applied. The emitting ions are then well embedded in the host matrix which remains identical. As a consequence, the nonradiative probability is not changed. In addition, the model cited just before supposes an electric-dipole transition. We thus used the intense $^5D_0 \rightarrow {}^7F_2$ transition of Eu^{3+} ions located at C_2 sites. Indeed, the crystal field in the C_2 symmetry site allows a forced electric-dipole transition within the $4f^6$ configuration.

The structural properties have been analyzed by transmission electron microscopy (TEM) with a Topcom EM-002B microscope, working at 200 kV. Cross-section images have been obtained with a cleaved sample consisting of the emitting film covered with 23 TiO_2 layers (Fig. 1). The films appear homogenous and their thicknesses are equal to 43 ± 2 nm for the $Eu^{3+}:Gd_2O_3$ layer and 417 ± 2 nm for the TiO_2 one. From the electron diffraction of each layer and high-resolution transmission electron microscopy (HRTEM) images, the $Eu^{3+}:Gd_2O_3$ layer appears crystallized in the cubic phase whereas the TiO_2 layers are amorphous.

The precise measurements of the thickness and refractive index in both transverse electric and transverse magnetic polarizations were performed at each step of the process by *m*-lines spectroscopy[22] at 632.8 nm. The refractive index and thicknesses are calculated assuming a step index profile with at least two propagation modes in each polarization. For the first 13 TiO_2 layers, the TiO_2 layers have been deposited on the sample and at the same time on an additional sample with an already deposited TiO_2 film in order to get sufficient thickness to get propagating modes. Above 13 layers the *m*-line measurements were performed directly on the sample by subtracting the Gd_2O_3 layer thickness deduced from the TEM image. The average thickness of one TiO_2 layer is equal to (18 ± 1) nm. The thickness of the 23 layers is evaluated to 414 nm, which is in very good agreement with the TEM results. The mean refractive index of the amorphous TiO_2 film is 2.01.

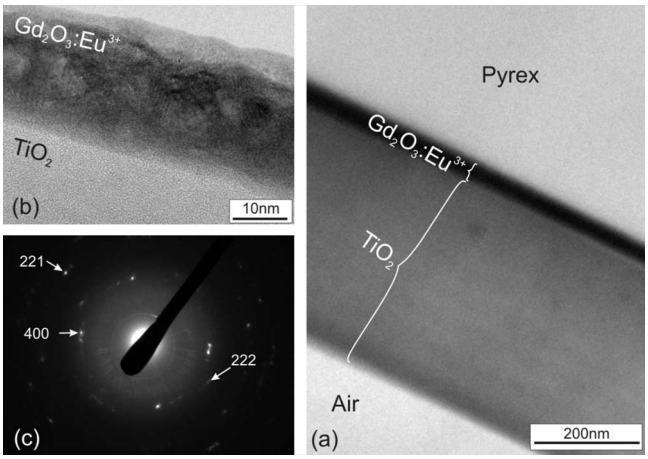

FIG. 1. TEM images of the layers structure at the end of the process. (a) Bright field image, (b) HRTEM image which shows crystal planes of Gd_2O_3 while TiO_2 is clearly amorphous, and (c) diffraction pattern of the Gd_2O_3 layer.

The emission spectra and fluorescence decays are recorded at room temperature by exciting the $^7F_0$ to $^5D_0$ transition at 580.4 nm with a dye laser pumped by a pulsed XeCl excimer laser. The fluorescence is analyzed by a monochromator with a 0.8 nm resolution and registered through a cooled AsGa photomultiplier by a photon-counting system or a multichannel counter.

The fluorescence spectra of Eu^{3+} ions confirm the crystallization in the cubic phase of the emitting layer and that no change is produced as TiO_2 layers are added. The measured photoluminescence (PL) decays ($\lambda_{em}=611.6$ nm) are presented on Fig. 2. Using a stretched exponential fitting procedure, an average PL decay time $\bar{\tau}$ is derived

$$\bar{\tau} = \frac{1}{I_0}\int_0^\infty I_{\mathrm{PL}}(t)dt \quad \text{with} \quad I_{\mathrm{PL}} = I_0 \times e^{-(t/\tau)^\beta}, \tag{1}$$

where I_0, τ, and β are the three parameters of the fit.

In Eq. (1) the measured β parameter varies between 0.82 and 0.89 which is not far from 1 (pure exponential behavior). This weak nonexponentiality may be explained by the various locations of the emitting centers within the film and therefore some changes of the local-field effect. To obtain a

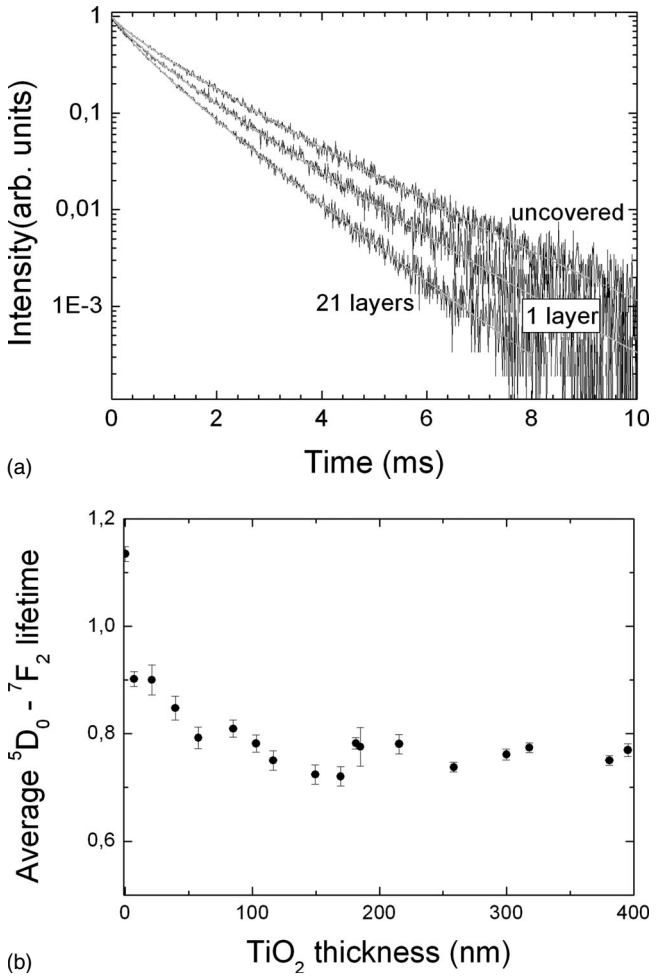

FIG. 2. (a) Decay time measurements for uncovered film 1 and 21 deposited TiO_2 layers. (b) Evolution of the decay time for the complete set of deposited layers. It corresponds to the τ parameter in the fitting procedure.

correct fitting ($R^2 \geq 0.99$) one has to give more weight to the behavior at longer times, so we fitted the logarithms of the decay curve.

Many studies report the disagreement between the predictions of models derived from Fermi's golden rules and the experimental results obtained by the emission analysis of nanoparticules inserted in different surrounding media.[11,13] In fact the empty cavity (EC) model (named also real cavity model in some papers[23]) [Eq. (2)] and the most recent fully microscopic (FM) model developed by Crenshaw and Bowden[24] [Eq. (3)] provide the best fits of the experimental data. By comparing the data from the literature, Duan *et al.*[25] draw general rules for selecting the appropriate model for a given emitting material. Since we are in the substitutional case ($Eu^{3+}-Gd^{3+}$), and based on their conclusions, the empty cavity model is probably the most appropriate.

$$\tau_{\mathrm{rad}}(n) = \left(\frac{3n^2}{2n^2+1}\right)^{-2} \frac{\tau_{\mathrm{vac}}}{n}, \tag{2}$$

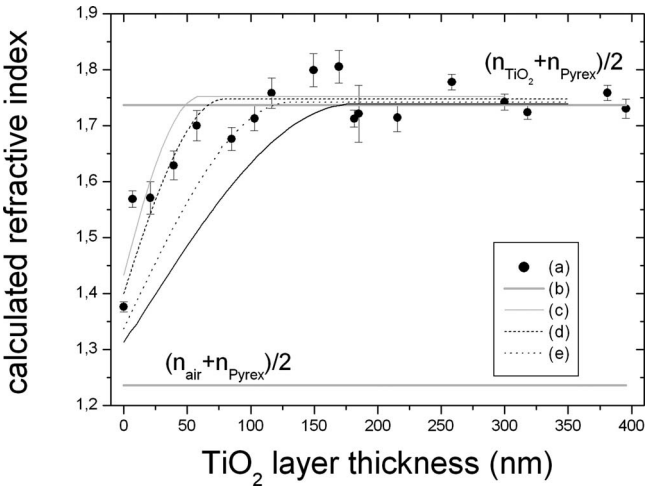

FIG. 3. (a) Refractive index deduced from the lifetime measurements as a function of the TiO_2 deposited thickness. Calculated refractive index considering an influence spheres whose radii are equal to (b) 80 nm, (c) 100 nm, (d) 150 nm, and (e) 200 nm.

$$\tau_{\mathrm{rad}}(n) = \left(\frac{n^2+2}{3}\right)^{-1} \tau_{\mathrm{vac}}. \tag{3}$$

In our sample the evaluation of the refractive index around the emitters is more difficult. The first step of our analysis consists in considering the two extreme situations: before any TiO_2 layer deposition (the average index of refraction seen by the layer is then $n_{\mathrm{avg}}=\frac{n_{\mathrm{pyrex}}+n_{\mathrm{air}}}{2}$) and after a thick TiO_2 layer deposition ($n_{\mathrm{avg}}=\frac{n_{\mathrm{pyrex}}+n_{\mathrm{TiO_2}}}{2}$). For this second case, we evaluated the mean radiative lifetime as 0.76 ms once the decay time remains unchanged when additional layers are added. By using the EC and FM models, the calculated τ_{vac} radiative lifetimes in vacuum calculated are 2.19 and 1.27 ms, respectively. The first value corresponds exactly to the value obtained in Ref. 23. Note that this value assumes a quantum efficiency of 100%. It is known that Eu^{3+} is a very efficient luminescent ion exhibiting a quantum yield near to 1 due to the lack of nonradiative process from the emitting level $^5D_0$. A quantum yield about 100% under UV excitation has been measured in the similar material $Y_2O_3:Eu^{3+}$ by Berkowitz and Olsen.[26] In order to check the effect of a potential lower quantum efficiency in our system, we calculated that even with a quantum efficiency of 90%, $\tau_{\mathrm{vac}}=2.44$ ms with the EC model. Therefore the EC model has been used to deduce the refractive index from the measured decay lifetime as a function of the TiO_2 layer thickness (Fig. 2). For thicknesses above 150 nm the refractive index felt by the emitters does not change. So this stabilization establishes experimentally the limit distance discussed before $d \ll \lambda$.

However another way to estimate the local refractive index could be by using the Bruggeman effective-medium approximation[1] applied to a sphere of radius R centered at the middle of the Gd_2O_3 emitting layer and considering $\tau_{\mathrm{vac}}=2.19$ ms. The refractive index and the volume of the

different elements contained in this sphere have been calculated using the data measured by *m*-lines spectroscopy and TEM analysis. The evolution of refractive index for different values of R are plotted in Fig. 3. The best agreement is observed for R between 100 and 150 nm, which corresponds to about $\lambda/4$ with λ equal to the emission wavelength in air (611.6 nm).

In conclusion, using a luminescent nanofilm as a probe, we measured the smallest elementary volume which has to be considered around a given position for the calculation of the local refractive index. This volume corresponds to a sphere of radius about $\lambda/4$. The next step of this study will be to check the agreement between the R value we found and the fluorescence wavelength by using other probes exhibiting multiple emission wavelength.

The authors want to thank R. S. Meltzer from the University of Georgia, Athens, for the fruitful discussions.

*Corresponding author; dujardin@pcml.univ-lyon.fr

[1] D. E. Aspnes, Am. J. Phys. **50**, 704 (1982).
[2] G. Russakoff, Am. J. Phys. **38**, 1188 (1970).
[3] H. A. Lorentz, *Versuch einer Theorie der elektrischen und optischen Erscheinungen in bewegten Körpern*, Elibron Classics Series 2005 (Replica of Edition published by E. J. Brill, Leiden, 1895).
[4] Z. Hashin and S. Shtrikman, J. Appl. Phys. **33**, 3125 (1962); D. J. Bergman, Phys. Rev. Lett. **44**, 1285 (1980); Phys. Rev. B **23**, 3058 (1981); G. W. Milton, J. Appl. Phys. **52**, 5286 (1981).
[5] D. E. Aspnes, Thin Solid Films **89**, 249 (1982).
[6] D. E. Aspnes, Phys. Rev. Lett. **48**, 1629 (1982).
[7] W. Egan and D. Aspnes, Phys. Rev. B **26**, 5313 (1982).
[8] D. Aspnes, Phys. Rev. B **25**, 1358 (1982).
[9] G. Nienhuis and C. Alkemade, Physica B & C **81**, 181 (1976).
[10] G. Lamouche, P. Lavallard, and T. Gacoin, Phys. Rev. A **59**, 4668 (1999).
[11] S. F. Wuister, C. M. Donega, and A. Meijerink, J. Chem. Phys. **121**, 4310 (2004).
[12] R. S. Meltzer, S. P. Feofilov, B. Tissue, and H. B. Yuan, Phys. Rev. B **60**, R14012 (1999).
[13] K. Dolgaleva, R. W. Boyd, and R. W. Milonni, J. Opt. Soc. Am. B **24**, 516 (2007).
[14] E. Yablonovitch, T. J. Gmitter, and R. Bhat, Phys. Rev. Lett. **61**, 2546 (1988).
[15] H. Yokoyama, K. Nishi, T. Anan, H. Yamada, S. D. Brorson, and E. P. Ippen, Appl. Phys. Lett. **57**, 2814 (1990); B. Ohnesorge, M. Bayer, A. Forchel, J. P. Reithmaier, N. A. Gippius, and S. G. Tikhodeev, Phys. Rev. B **56**, R4367 (1997); G. S. Solomon, M. Pelton, and Y. Yamamoto, Phys. Rev. Lett. **86**, 3903 (2001).
[16] K. E. Kunz and W. Lukosz, Phys. Rev. B **21**, 4814 (1980); K. H. Drexhage, J. Lumin. **1-2**, 693 (1970).
[17] G. L. J. A. Rikken, Phys. Rev. A **51**, 4906 (1995); H. P. Urbach and G. L. J. A. Rikken, *ibid.* **57**, 3913 (1998).
[18] S. D. Brorson, H. Yokoyama, and E. P. Ippen, IEEE J. Quantum Electron. **26**, 1492 (1990).
[19] I. Abram, I. Robert, and R. Kuszelewicz, IEEE J. Quantum Electron. **34**, 71 (1998).
[20] A. Garcia-Murillo, C. L. Luyer, C. Garapon, C. Dujardin, E. Bernstein, C. Pedrini, and J. Mugnier, Opt. Mater. (Amsterdam, Neth.) **19**, 161 (2002).
[21] A. Bathat, M. Bonazaoui, M. Bathat, C. Garapon, B. Jacquier, and J. Mugnier, J. Non-Cryst. Solids **202**, 16 (1996).
[22] R. Ulrich and R. Torge, Appl. Opt. **12**, 2901 (1973).
[23] F. J. P. Schuurmans, D. T. N. de Lang, G. H. Wegdam, R. Sprik, and A. Lagendijk, Phys. Rev. Lett. **80**, 5077 (1998).
[24] M. E. Crenshaw and C. M. Bowden, Phys. Rev. Lett. **85**, 1851 (2000).
[25] Chang-K. Duan, M. F. Reid, and Z. Wang, Phys. Lett. A **343**, 474 (2005).
[26] J. K. Berkowitz and J. A. Olsen, J. Lumin. **50**, 111 (1991).